



Surface integrity and fatigue behaviour of electric discharged machined and milled austenitic stainless steel



Mattias Lundberg*, Jonas Saarimäki, Johan J. Moverare, Mattias Calmunger

Division of Engineering Materials, Department of Management and Engineering, Linköping University, SE-581 83 Linköping, Sweden

ARTICLE INFO

Article history:

Received 2 May 2016

Received in revised form 3 January 2017

Accepted 3 January 2017

Available online 05 January 2017

Keywords:

Austenitic stainless steel

Fatigue

Surface integrity

SEM

XRD

Hardness

ABSTRACT

Machining of austenitic stainless steels can result in different surface integrities and different machining process parameters will have a great impact on the component fatigue life. Understanding how machining processes affect the cyclic behaviour and microstructure are of outmost importance in order to improve existing and new life estimation models. Milling and electrical discharge machining (EDM) have been used to manufacture rectangular four-point bend fatigue test samples; subjected to high cycle fatigue. Before fatigue testing, surface integrity characterisation of the two surface conditions was conducted using scanning electron microscopy, surface roughness, residual stress profiles, and hardness profiles. Differences in cyclic behaviour were observed between the two surface conditions by the fatigue testing. The milled samples exhibited a fatigue limit. EDM samples did not show the same behaviour due to ratcheting. Recrystallized nano sized grains were identified at the severely plastically deformed surface of the milled samples. Large amounts of bent mechanical twins were observed $\sim 5 \mu\text{m}$ below the surface. Grain shearing and subsequent grain rotation from milling bent the mechanical twins. EDM samples showed much less plastic deformation at the surface. Surface tensile residual stresses of $\sim 500 \text{ MPa}$ and $\sim 200 \text{ MPa}$ for the milled and EDM samples respectively were measured.

© 2017 Elsevier Inc. All rights reserved.

1. Introduction

Stainless steels are used in various industries such as aerospace, automotive, biomedical, and power generation. Due to its wide field of use, extensive research has been conducted in order to improve the mechanical properties and performance of stainless steels. Manufacturing a component to the required geometrical tolerances without the use of any machining is next too impossible. All types of machining e.g., milling, turning, drilling, plasma machining, laser cutting, water jet cutting, and electrical discharge machining (EDM) results in different surface integrities, resulting in different mechanical behaviour. Optimising machining parameters in order to minimise machining time without compromising surface quality and/or given geometrical tolerances have been investigated in [1]. Different surface conditions can alter the mechanical behaviour during cyclic loading and influence fatigue life of AISI 304 and AISI 316 stainless steels [2–13]. To counteract the possibly detrimental effects that might be induced by machining, post treatments can be used to increase fatigue resistance and component life. A common way to achieve this is to altering the surface integrity by e.g., introducing an increased strain hardened layer, grain fragmentation and/or residual stress (RS) optimisation [7,14–16]. Commonly used surface processing techniques in industry today are shot

peening, laser shock peening, surface mechanical attrition treatment and deep rolling. Machining and surface treatments can alter mechanical properties such as fatigue strength. Therefore, it is essential to understand the microstructural evolution at the surface and its impact on fatigue resistance [17–20]. Four-point bending fatigue testing may be a suitable fatigue testing method to study the surface integrity after machining, since the highest stresses from testing will be concentrated at the sample surface.

This study investigates the effect of milling and EDM on high cycle fatigue of AISI 304 austenitic stainless steel tube material. Fatigue resistance in relation to surface integrity is investigated using the scanning electron microscopy (SEM) techniques, electron channelling contrast imaging (ECCI), electron backscatter diffraction (EBSD), and energy dispersion spectroscopy (EDS), and hardness testing, and RS measurements using X-ray diffraction (XRD).

2. Material and Experimental Procedure

The AISI 304 austenitic stainless steel used for this study was provided by Sandvik Materials Technology in Sandviken, Sweden. The tube material was manufactured by hot extrusion cold pilgering and solution annealed at $1060 \text{ }^\circ\text{C}$ for 15 min. Chemical composition of the steel in weight percentage is C: 0.015, Si: 0.35, Mn: 1.2, Cr: 18.3, Ni: 10.3, W: 0.05, Cu: 0.3, Nb: 0.01, N: 0.07, and balance Fe. The mechanical

* Corresponding author.

E-mail address: mattias.lundberg@liu.se (M. Lundberg).

properties were i.e., yield strength, $R_{p0.2} = 210$ MPa, tensile strength, $R_m = 515$ MPa, Young's modulus, $E = 200$ GPa.

Ten rectangular shaped samples were extracted from the tube using milling and EDM respectively. Milling was performed with coolant and a Sandvik Model 390 cutting tool with a ϕ of 16 mm and new inserts, 0.8 mm nose radius, rotation speed of 1200 rpm and a feed rate of 200 mm/min. A schematic sketch of the milling process is shown in Fig. 1(a). EDM was performed using a ϕ 0.25 mm brass wire with a cutting speed of 7.6 mm/min, 50 V, and 4.0 A. Surface roughness, R_a , measurements were conducted using a Mitutoyo Surftest SJ-201M. Measurements of the milled and the EDM surface had a R_a value of 0.81 and 2.27 respectively.

2.1. Fatigue Testing

Four-point bending fatigue testing was done in a servo-hydraulic MTS machine using an Instron 8800 control system with a frequency of 15 Hz and a load ratio of $R = 0.1$. The experimental setup is shown in Fig. 1(b). To fulfil the recommendations by Zhai et al. [21], samples measuring $10 \times 10 \times 80$ mm, an inner span of 13 mm, and an outer span of 58 mm for the test setup were used. A drop in displacement of 3.5% was used as the failure criterion. A test was considered a run-out (RO) if exceeding two million cycles.

2.2. Hardness Testing and X-ray Diffraction

A Struers DuraScan G5, following ISO 6507 and ASTM E384, equipped with a Vickers diamond was used for hardness measurements with an applied load of 0.01 g. For hardness depth profiles 65 and 30 indentations were used for the milled and EDM samples respectively. Bulk hardness was measured using 35 indentations.

X-ray measurements were performed using a four-circle goniometer Seifert X-ray machine, equipped with a linear position sensitive detector and a Cr-tube. RS evaluations were conducted using the $\sin^2\psi$ -method [22] with the γ -Fe {220} diffraction peak, at $2\theta \approx 128.8^\circ$. X-ray elastic constants s_1 and $1/2s_2$ were taken from reference [23]. The RS measurements conducted, used nine equally spread $\sin^2\psi$ values with ψ -angles between $\pm 55^\circ$. Material removal was done using a perchloric acid-base electrolyte in a Struers LetcroPol-5 machine. No corrections were done for material removed.

2.3. Microscopy

Samples were prepared by grinding and mechanical polishing using a Struers Tegramin machine with the parameter settings in Table 1. Samples were cleaned using water, soap and cotton after each grinding operation. After each polishing cloth they were cleaned with water, soap and cotton followed by ultrasonic cleaning in ethanol and a final cleaning with water, soap and cotton. A Hitachi SU-70 field emission gun SEM, operating at 10–20 kV, was used to study the sample surface integrity and deformation caused by the different cutting procedures. The analytical SEM-techniques used were ECCI, EBSD, and EDS.

ECCI investigations were performed using a solid state 4-quadrant backscatter electron detector, an acceleration voltage of 10–20 kV, and a working distance of 7–8 mm. Changes in the crystallographic structure

gives the speckled pattern observed with ECCI [24–26]. The probability of detecting back scattering electrons varies with the rotational changes around any axis of the crystal. Local mis-orientation, defects, and strain fields are shown as contrast variations because ECCI uses the interaction between backscattered electrons and the crystal planes to generate contrast. This makes ECCI a good technique in order to investigate deformed materials [24–26]. It is not possible to separate or quantify the contributions from elastic and plastic strain when simultaneously present.

Crystallographic orientation quantification was done using an OXFORD electron backscatter diffraction (EBSD) detector. Sample configuration used: tilted 70° , a working distance of 20 mm, an acceleration voltage of 15 kV and a step size of 0.5 μm . To evaluate the EBSD measurements the HKL software Channel 5 was used. A mis-orientation (orientation difference between two neighbouring measurement points) between 1.5° and 10° defines a LAGB while $>10^\circ$ is regarded as a high angle grain boundary. In the EBSD maps LAGBs are represented with black lines, angles between 10° and 50° are with red lines, and angles $>50^\circ$ with blue lines. Non indexed points (zero solutions) are represented as white dots.

Qualitative chemical composition measurement was done using an OXFORD EDS detector at a working distance of 15 mm and an acceleration voltage of 20 kV.

3. Results

All milled samples were run-outs (RO) when tested with a maximum stress of 400, 410, 420, and 425 MPa. The two samples run with a maximum stress of 430 MPa failed after 346,500 and 776,000 cycles respectively. The EDM samples were RO for all tested loads. Fatigue testing results are listed in Table 2.

Position tracking at minimum load revealed a significant difference in material behaviour for the two surface conditions as shown in Fig. 2. The starting value (zero) originates from a starting load of 0.6 kN, then the averaged position at minimum load over 1000 cycles are plotted for each data point.

3.1. Hardness Testing and Residual Stress

Milling clearly increases the surface hardness as illustrated in Fig. 3. Bulk hardness was $HV_{0.01} 185 \pm 15$. No changes in hardness could be seen for the EDM sample. The $HV_{0.01}$ hardness for the EDM material was 196 ± 7 which is within the range of the bulk hardness.

Fig. 4 shows the biaxial stresses (solid lines) and FWHM-distribution (dashed lines) measured in three different orientations for both the milled (a) and EDM (b) sample. Post milling, the surface RS are ~ 500 MPa in tension and converges towards zero at a depth of approximately 30–40 μm . For the milled material FWHM starts at 1.2° at the surface and drops to 0.6° at a depth of 30 μm , after which the FWHM converges towards the bulk value of 0.35° . The EDM sample showed tensile RS of 200 MPa at the surface which converged close to zero at a depth of ~ 10 μm . After which, the mean RS value fluctuates around zero. FWHM at the surface was 0.75° and converged towards the un-affected bulk value.

3.2. Microscopy

Three distinct zones can often be identified in Fig. 5(b) after milling: the severe plastically deformed (SPD) zone, the heavily deformed zone, and the affected zone. Nano sized recrystallized grains measuring approximately $40 \times 90\text{--}75 \times 150$ nm in the SPD zone are shown in Fig. 6(a). The nano sized grains had the longest side parallel to the cutting direction. The heavily deformed zone consists of a mixture of deformation mechanisms in multiple directions and partially evolved nano sized grains as seen in Fig. 6(c). Bending of mechanical twins (MT) is exemplified in Fig. 6(d). The affected zone consists of everything from

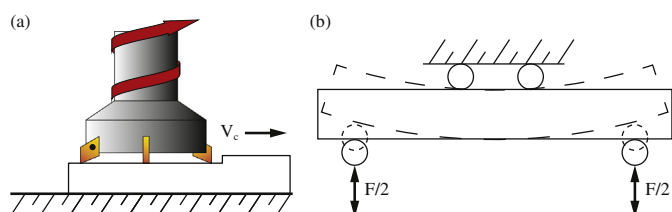


Fig. 1. Schematic sketch of the (a) milling process, and (b) four-point bending setup.

متن کامل مقاله

دریافت فوری ←

ISIArticles

مرجع مقالات تخصصی ایران

- ✓ امکان دانلود نسخه تمام متن مقالات انگلیسی
- ✓ امکان دانلود نسخه ترجمه شده مقالات
- ✓ پذیرش سفارش ترجمه تخصصی
- ✓ امکان جستجو در آرشیو جامعی از صدها موضوع و هزاران مقاله
- ✓ امکان دانلود رایگان ۲ صفحه اول هر مقاله
- ✓ امکان پرداخت اینترنتی با کلیه کارت های عضو شتاب
- ✓ دانلود فوری مقاله پس از پرداخت آنلاین
- ✓ پشتیبانی کامل خرید با بهره مندی از سیستم هوشمند رهگیری سفارشات